JEB™
Website : www.jeb.co.in
E-mail : editor@jeb.co.in

Journal of Environmental Biology

ISSN: 0254-8704 (Print)
ISSN: 2394-0379 (Online)
CODEN: JEBIDP

Decolorization of Reactive Red 238 and Reactive Blue 235 dyes by iron oxide nanoparticles synthesized using *Syzygium cumini* leaf extract

Elavarasi Natarajan* and Gomathi Priya Ponnaiah
Department of Chemical Engineering, A.C.College of Technology, Anna University, Chennai, 600025, India
*Corresponding Author E-mail: **elavarasijawahar@gmail.com**

Publication Info

Paper received:
13 October 2015

Revised received:
09 May 2016

Accepted:
5 November 2016

Abstract

Iron oxide nanoparticles were produced by a green synthetic route using an extract of *Syzygium cumini* leaves (bINP) and employed as a Fenton like catalyst for degradation of Reactive Red 238 (RR238) and Reactive Blue 235 (RB235), dye mix and wastewater collected from the textile dyeing industry. The synthesized nanoparticles were characterized by Fourier Transform Infra Red (FTIR) Spectroscopy, Scanning Electron Microscopy/ Energy Dispersive X-ray (SEM/ EDX) Analysis, Transmission Electron Microscopy (TEM) and X-ray Diffractometry (XRD). The decolorization efficiency of bINP was compared with iron oxide nanoparticles produced by borohydride reduction (cINP), using UV-visible spectroscopy. The degradation efficiency of bINP (2.0 gl^{-1}) towards RR238 and RB235 was found to be 100% and that of cINP was found to be 70% and 71%, respectively.

Key words

Dye decolorization, Iron oxide nanoparticles, *Syzygium cumini,* UV-Visible Spectroscopy

Introduction

The textile sector consumes about 60% of total dye production for coloration of various fabrics and out of it around 10-15% of the dyes used for coloration is discharged through the effluent (Rajkumar and Nagan, 2011). The discharge of highly colored effluent is aesthetically displeasing and can contaminate receiving water body by impeding penetration of light (Nigam, 2000). The most harmful compound in the textile dye effluents are the reactive dyes (Carliell *et al*., 1994; Carliell *et al*., 1996) as they are moderately resistant to degradation under natural conditions (Mukesh Chander *et al*., 2014). Among them, the family of reactive azo dyes is of special interest because they may produce aromatic amines under anaerobic conditions which are considered to be highly carcinogenic, mutagenic and toxic (Pinheiro *et al*., 2004; Frank *et al*., 2005). Elimination of dyes from the wastewater of textile industry is a main problem (Venkatesh *et al*., 2011) resulting in major environmental concerns concerning the intensity of color and organic properties such as chemical oxygen demand. Therefore, the extremely colored textile industry wastewater has to be decolorized by a proficient pretreatment method (Hung-Yee Shu *et al*., 2007).

The conventional textile effluent treatment methods such as biological processes are not very effective because most of the commercial dyes are non-biodegradable due to complex chemical structure (Garg *et al*., 2010; Bernal-Martinez *et al*., 2010) and do not show economic feasibility. Thus, oxidation processes such as direct oxidation processes and advanced oxidation processes are preferred to degrade the dyes. Advanced oxidation processes typically operate with less energy requirement than direct oxidation, and reduces the chemical contaminants and their toxicity to such an extent that cleaned wastewater may be reintroduced in the

Online Copy

receiving streams (Arjunan and Karuppan, 2014).

In Fenton process, hydrogen peroxide reacts with iron ions to form reactive oxygen species that has been used for the treatment of azo dyes containing wastewater. But huge quantities of sludge and high concentration of anions are formed during this process (Byung *et al*., 2011). An alternative process to overcome these disadvantages is to use zero valent iron (ZVI) as iron source, instead of ferrous ion (Tang and Chen, 1996). Recently, the use of iron nanoparticles has been reported to decolorize dye solution as it can exhibit high reactivity because of its extremely small particle size and large surface area (Byung *et al*., 2011). The advantages of iron nanoparticles for dye color removal is ease of operation, as well as recycling of spent iron particles by magnetism; additionally the effluent has no further treatment demand due to remaining low iron concentration (Chang *et al*., 2006). The iron nanoparticles can be synthesized by many chemical and physical methods. Aggregation of these nanoparticles into chain like structures is one of their well-known characteristics that reduce the surface area to volume ratio (Sun *et al*., 2007). These methods also employ toxic chemicals as reducing agents, organic solvents, or non-biodegradable stabilizing agents and are therefore, potentially dangerous to the environment and biological systems. Moreover, most of them entail intricate controls or nonstandard conditions making them quite expensive.

A cost-effective environment-friendly alternative to chemical and physical methods is the biosynthesis of nanoparticles. Consequently, nanomaterials have been synthesized using microorganisms and plant extracts. The use of plant extracts for the synthesis of nanoparticles is potentially advantageous over microorganisms due to the ease of scale up and eliminate the elaborate process of maintaining cell cultures (Eric *et al*., 2011).The plant mediated synthesis is an economically valuable and environmentally benign alternative for the large-scale production of metal nanoparticles as biomolecules present in the plant extract may act both as reducing and capping agent (Siavash Iravani, 2011).

In the present study, green synthesis of iron oxide nanoparticles using *Syzygium cumini* leaf extract, as both reducing and capping agent, was reported. *Syzygium cumini* is native to the parts of South and Southeast Asia (Sada Venkateswarlu *et al*., 2014) and is widely available throughout India and the drier parts of Southeast Asia, Malaya, East Indies and tropical Africa. *Syzygium cumini* is a rich source of polyphenols (Bajpai *et al*., 2005) which has been reported to play a vital function in the synthesis of nanoparticles (Vineet Kumar *et al*., 2010) by acting both as reducing and capping agent.

In view of the above, the present study was carried out to compare the efficiency of bINP and cINP in the presence of H_2O_2 to decolorize RR238, RB235, dye mix, and wastewater collected from the textile dyeing industry.

Materials and Methods

RR238, RB235 and wastewater containing both RR238 and RB235 were obtained from a textile dyeing industry in Tirupur District, Tamilnadu, (India). Both are commercial reactive azo dyes of new generation, employed in cellulosic fabric dyeing process.

Preparation of bINP : *Syzygium cumini* leaves were collected locally and shade dried for 30 days. Equal volume of 1% w/v of ferrous oxalate solution in deionized water was added to 2% w/v of *S. cumini* aqueous leaf extract using a separating funnel @ 1 ~ 2 drops per second. The mixture was incubated for 1 hr at room temperature. Synthesis of bINP was marked by the appearance of black precipitate that was centrifuged for 4 min at 4000 rpm and then dried for 6 hrs at 100°C in a hot air oven.

Preparation of cINP : cINP was prepared using 2% w/v sodium borohydride as reducing agent by a method similar to bINP synthesis. cINP was washed thrice with 10^{-4} N HCl (Changha Lee *et al*., 2008).

Characterization of iron oxide nanoparticles (INP): The FT-IR spectrum in the range of 4000 to 450 cm^{-1} was recorded using a Perkin Elmer Spectrum One FTIR spectrometer using KBr pellet at 1.0 cm^{-1} resolution. The surface morphology of INP was observed by F E I Quanta FEG 200 - High-Resolution Scanning Electron Microscope. The elemental composition was analyzed by energy dispersive X-ray elemental analysis equipped with SEM instrument. Transmission electron microscopy (TEM) image of INP was acquired on JOEL- JEM 1400 TEM operating at 80 kV. The XRD analysis was recorded using X-ray diffraction (Rigaku) with CuKα radiation (1.5406 Å) in the 2θ scan range of 20-50°. The average crystallite size of nanoparticles was calculated from the lower full-width-at-half maximum (FWHM) of most intense XRD peaks using Scherrer's equation:

$$D = 0.9\lambda/\beta \cos\theta \qquad (1)$$

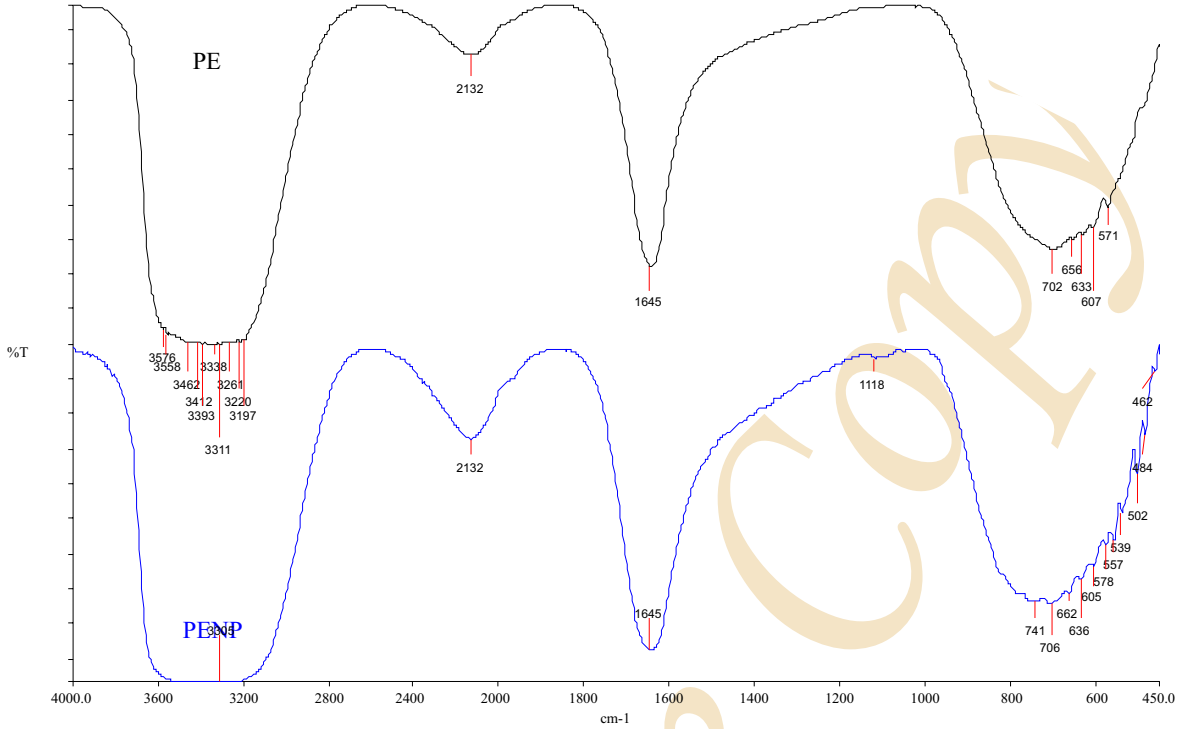

Fig. 1 : FTIR spectrum of *Syzygium cumini* leaf extract (PE) and green synthesized iron oxide nanoparticles (PENP)

where, D is the particle size; λ is the X-ray wavelength (nm); θ is Bragg's angle and β is the excess line broadening (radiant).

Effect of bINP and cINP concentration on decolorization of RR238, RB235 and dye mix : A 45 ml of aqueous dye solution (50 mgl^{-1}) and 5 ml of 10% H_2O_2 was poured into a 250 ml Erlenmeyer flask, and 0.4, 0.8, 1.2, 1.6 or 2.0 gl^{-1} of bINP or cINP was added. The flasks were shaken at 150 rpm by an orbital shaker. All the experiments were performed thrice at 25°C at atmospheric pressure. Aliquots of samples were collected every 10 min for 200 min and centrifuged at 10,000 rpm for 3 min. The residual dye concentrations were quantified by UV- Visible double beam spectrophotometer at 543 nm, 605nm and 575nm for RR238, RB235 and dye mix, respectively. The rate of dye degradation, K_{obs} (hr^{-1}) was determined from the slope of a linear relationship obtained by plotting ln (A_0/A_t) vs time which indicates the first order reaction given by equation (2).

$$\ln A_0/ A_t = K_{obs}.t \qquad (2)$$

where, A_t is the absorbance at time = t and A_0 is the absorbance at t = 0.

The percentage of dye removal (DR %) at time 't' was calculated by using equation:

$$DR\ \% = \frac{A_0-A_t}{A_0} X\ 100 \qquad (3)$$

Decolorization of dyes in wastewater : A 45 ml of wastewater and 5 ml of 10% H_2O_2 were poured into a 250 ml Erlenmeyer flask, and 2.0 gl^{-1} of bINP or cINP was added. The samples were collected every 10 min for 100 min and centrifuged at 10,000 rpm for 3 min.

Results and Discussion

Characterization of bINP and cINP : FTIR spectral analysis was performed to identify the functional groups involved in the synthesis of bINP. Fig. 1 shows the FTIR spectrum of plant extract and green synthesized iron nanoparticles. In FTIR spectrum of plant extract, a broad band with several peaks were observed between 3800 to 3000 cm^{-1} that were due to phenolic hydroxyl (O-H) stretch, whereas in bINP a single peak at 3305 cm^{-1} was observed. A

Online Copy

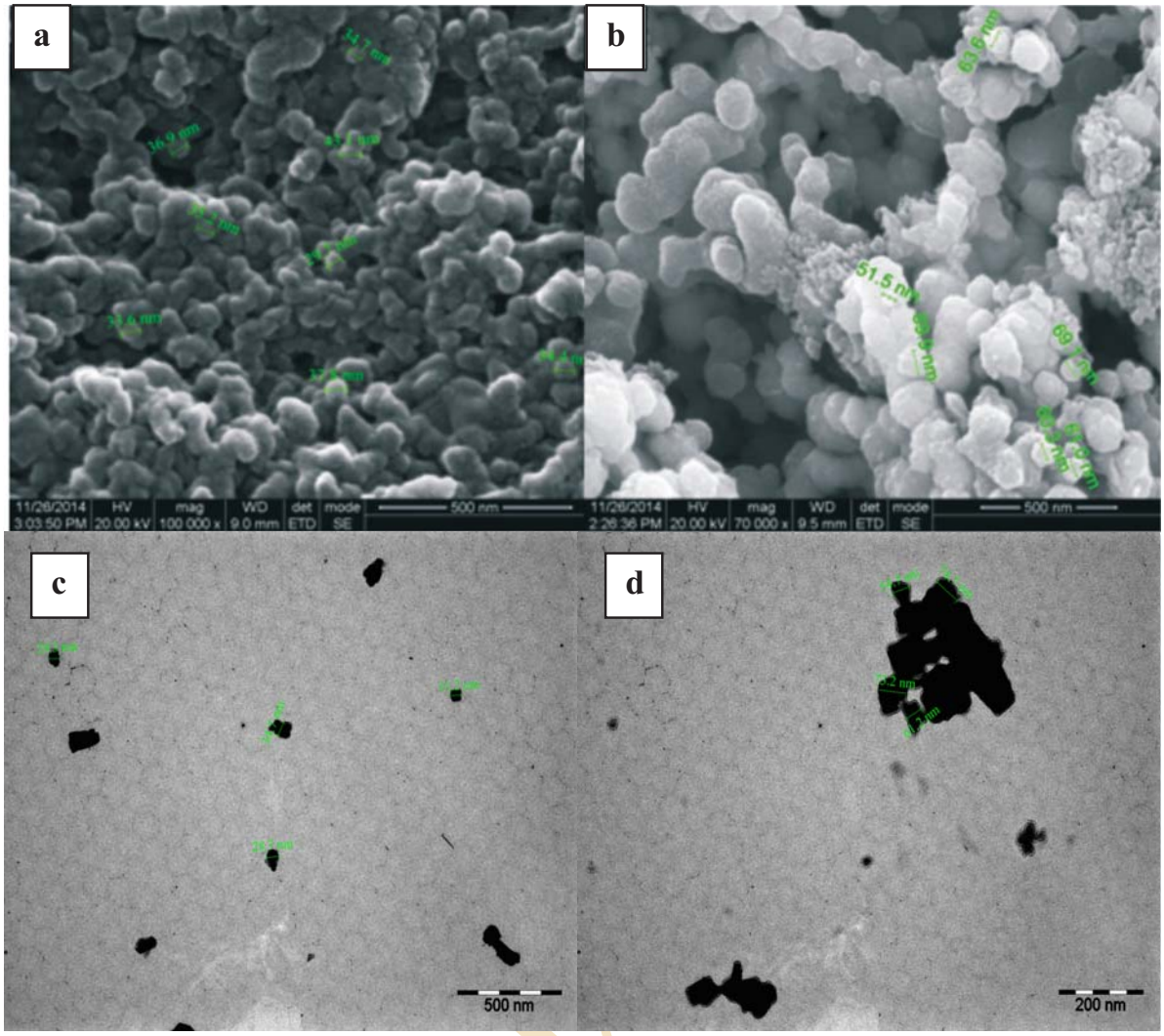

Fig. 2 : (a) SEM image of bINP, (b) SEM image of cINP, (c)TEM image of bINP and (d) TEM image of cINP

peak at 2132 cm^{-1} represented the –C≡C– stretch, and another at 1644 cm^{-1} corresponded to primary amine groups, respectively. A peak between 800 and 450 cm^{-1} corresponded to Fe-O stretching bands. Results suggest that polyphenols with bound amide region could be involved in bINP synthesis (Krishnan and Maru, 2006; Máirtín *et al*., 2003; Susanto *et al*., 2009).

Information about the morphology of the products was studied by SEM at a magnification of 500 nm (Fig 2a, 2b), and TEM at 200 nm with an accelerating voltage of 80 kV (Fig 2c, 2d). The SEM images suggest that the nanoparticles prepared by both the methods were found to be irregular in shape. The SEM micrographs revealed that the average size of bINP was 35.67±3.60 nm and that of cINP was 66.05±11.87 nm. TEM micrograph of bINP showed that they were irregularly shaped and well separated from each other with an average size of 31.87±4.65 nm, whereas cINP agglomerated to form irregular clusters with an average size of 66.45±8.806 nm.

EDX analysis was employed to examine the chemical composition of the INPs (Fig 3). The spectra of bINP and cINP contained intense peaks of Fe and O. Na signal might

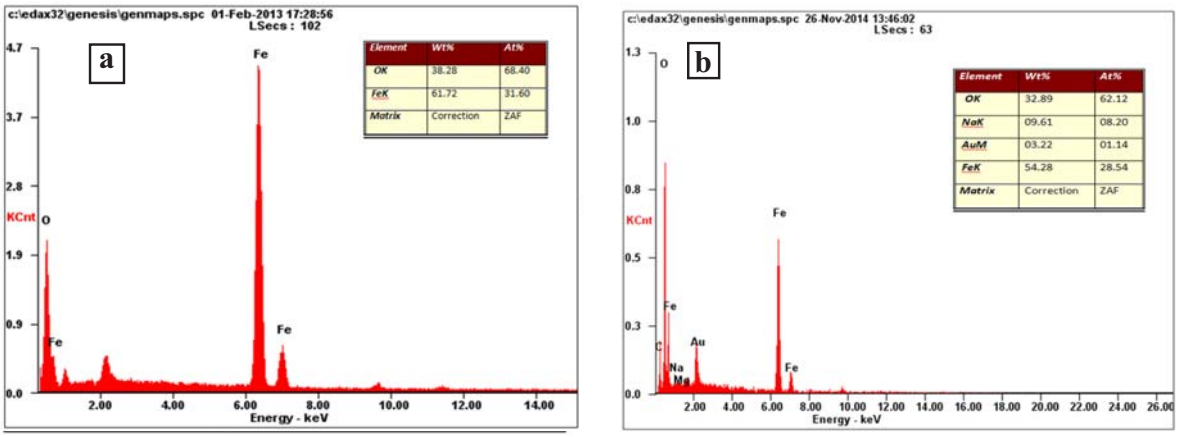

Fig. 3 : (a) EDAX spectrum of bINP and (b) EDAX spectrum of cINP with inset showing elemental composition

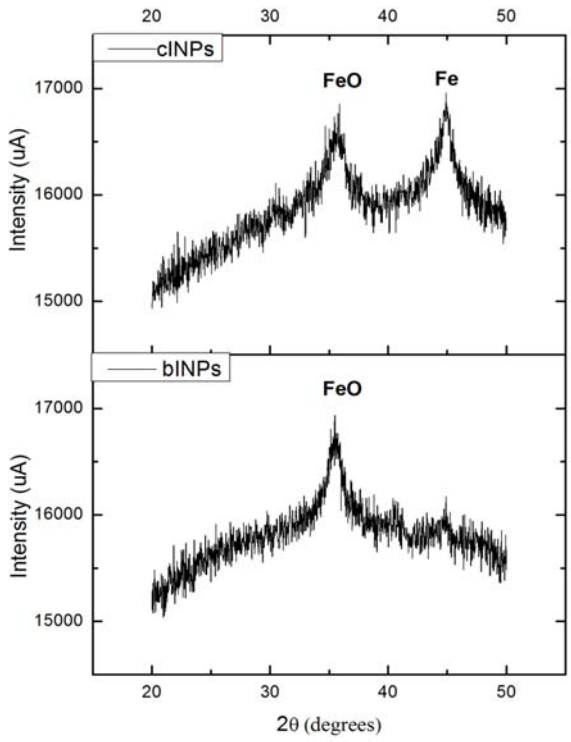

Fig. 4 : XRD patterns of bINP and cINP

have originated from $NaBH_4$ used in synthesis of cINP, and Au signal was attributed to gold used for sputtering the sample in SEM/EDX analysis. The weight percentages of bINP and cINP, as obtained by EDX quantification, was 38.28 % Fe, 61.72 % O and 32.89 % Fe , 54.28% O, 9.61% Na and 3.22% Au, respectively.

The XRD pattern of bINP and cINP is shown in Fig. 4. The XRD peak of bINP at 2θ of 35.5° was found to be in agreement with those of previously reported 2θ value of tetragonal γ- iron oxide (JCPDS Card No.89-5894), and the diffraction peaks of cINP observed at 2θ of 44.9° and 35.9° indicated the presence of both zero-valent iron (α-Fe) and cubic, face-centered iron oxide (JCPDS Card No.89-0687) (Sun *et al*., 2006). The particle size of bINP was found to be 29 nm and that of cINP was found to be 58 nm according to Debye-Scherrer formula using full width at half maximum of the diffracted beam.

Effect of bINP and cINP dosage on decolorization of RR 238, RB 235 and dye mix : Fenton process encompasses the reaction of peroxides such as hydrogen peroxide with Fe^{2+} ion generating hydroxyl radical (OH according to equation (4) and (5). The cleavage of azo bond (–N=N–) in the chromophore of reactive dyes by OH radical resulted in decolorization.

$$Fe^{2+} + H_2O_2 \rightarrow Fe^{3+} + OH^- + OH^- \quad (4)$$

$$Fe^{3+} + H_2O_2 \rightarrow Fe^{2+} + OOH + H^+ \quad (5)$$ (Shahwan *et al*., 2011)

To overcome the disadvantages of traditional Fenton process such as production of huge amount of sludge and formation of high concentration of anions, a better alternative would be use of iron nanoparticles as it can exhibit high reactivity because of its extremely small particle size and large surface area (Byung *et al*., 2011), and it is also possible to recycle spent iron nanoparticles by magnetism; additionally the effluent has no further treatment demand due

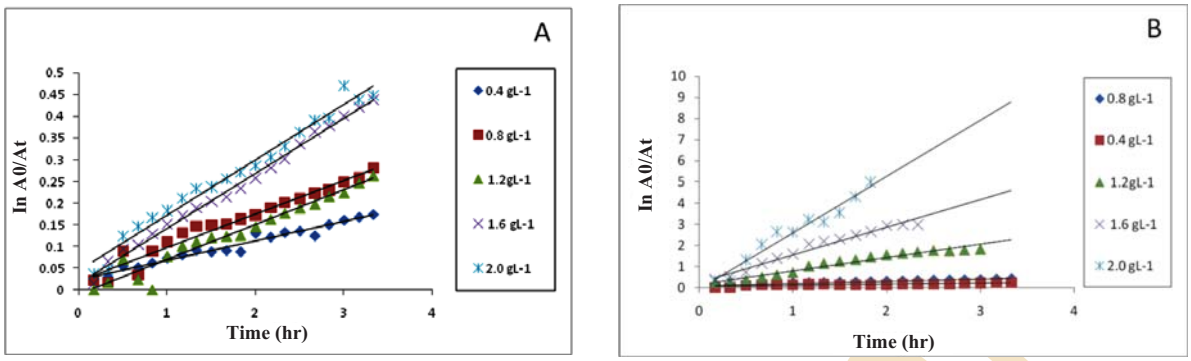

Fig. 5 : Kinetics of degradation of RR238 by cINP (A) and bINP (B) in the presence of H_2O_2

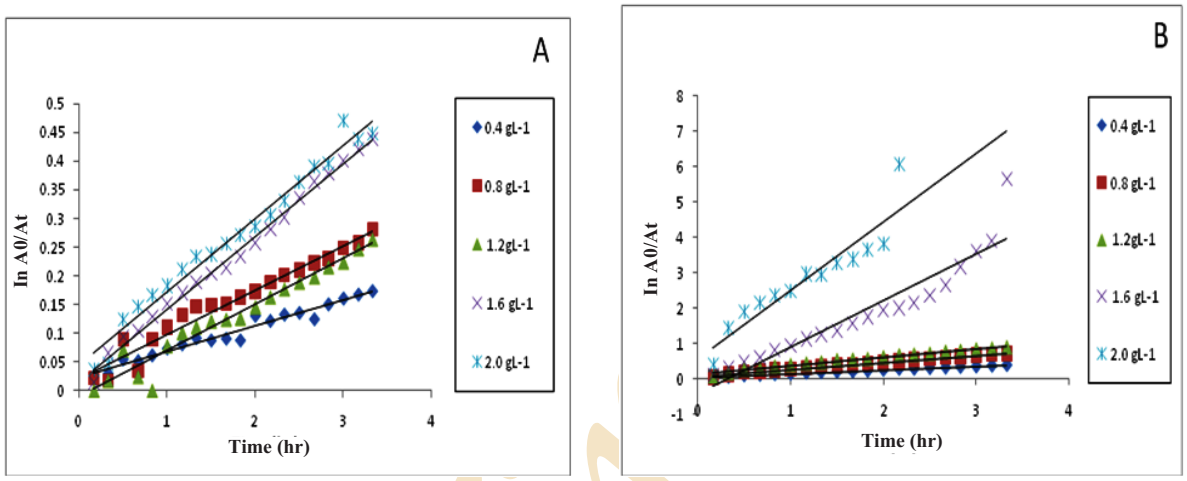

Fig. 6 : Kinetics of degradation of RB235 by cINP (A) and bINP (B) in the presence of H_2O_2

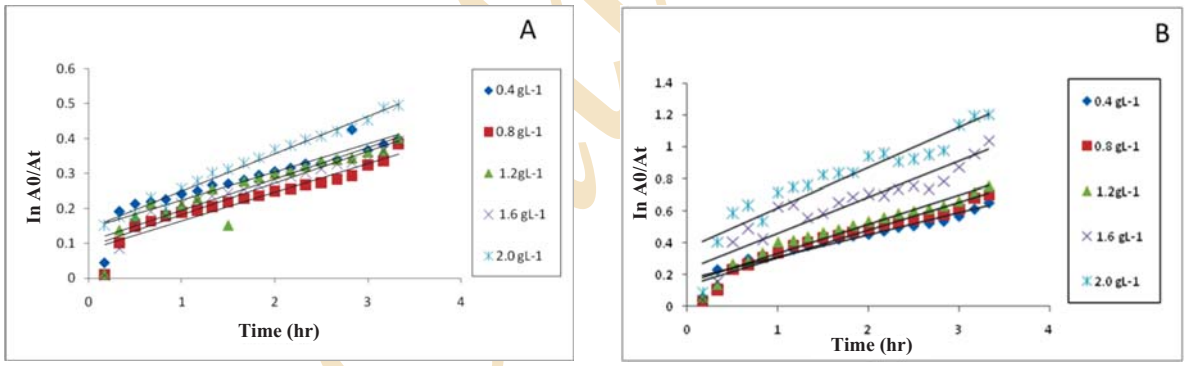

Fig. 7 : Kinetics of degradation of dye mix by cINP (A) and bINP (B) in the presence of H_2O_2

to remaining low iron concentration (Chang *et al*., 2006). Iron oxides, iron oxohydroxide, and zero valent iron nanoparticles can be used as a source of ferrous ions in Fenton like process (Shahwan *et al*., 2011).

The first order kinetic parameters of RR238, RB235 and dye mix degradation by different concentrations of bINP and cINP are presented in Fig. 5-7 and Table 1. When dose of nanoparticles increased, the K_{obs}

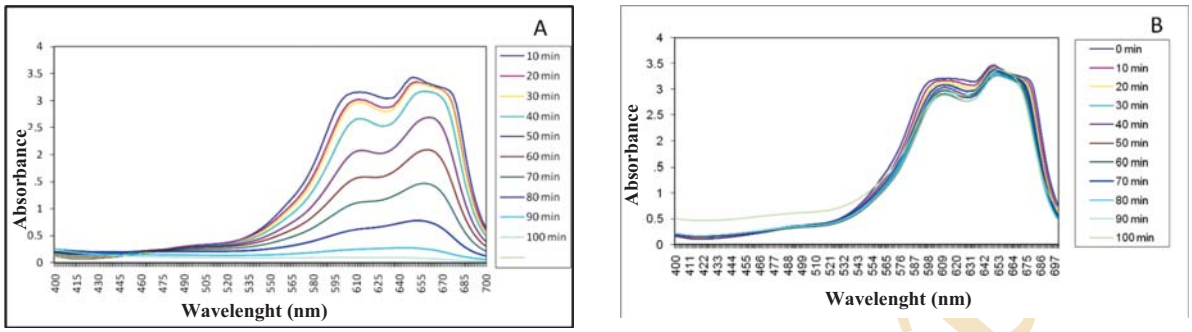

Fig. 8 : UV-visible spectra of textile industry wastewater treated by 2.0 gl^{-1} bINP (A) and cINP (B).

Table 1 : First order reaction kinetics parameters of RR238, RB235 and dye mix at different concentrations of bINP and cINP

Concentration	RR238				RB235				Dye mix			
(gl^{-1})	bINP		cINP		bINP		cINP		bINP		cINP	
	K_{obs} (hr^{-1})	R^2	K_{obs} (hr^{-1})	R^2	K_{obs} (hr^{-1})	R^2	K_{obs} (hr^{-1})	R^2	K_{obs} (hr^{-1})	R^2	K_{obs} (hr^{-1})	R^2
0.4	0.053	0.891	0.190	0.978	0.112	0.992	0.044	0.964	0.139	0.926	0.081	0.859
0.8	0.103	0.744	0.213	0.974	0.193	0.990	0.076	0.958	0.173	0.937	0.082	0.906
1.2	0.628	0.954	0.255	0.965	0.240	0.983	0.08	0.950	0.181	0.938	0.089	0.848
1.6	1.315	0.972	0.360	0.981	1.310	0.882	0.126	0.976	0.225	0.846	0.09	0.897
2.0	2.656	0.956	0.34	0.986	1.938	0.860	0.128	0.993	0.252	0.863	0.107	0.986

Table 2 : Dye removal % (DR%) of RR238, RB235 and dye mix at different concentrations of bINP and cINP

Concentration (gl^{-1})	DR% of RR238		DR% of RB235		DR% of Dye mi x	
	bINP	cINP	bINP	cINP	bINP	cINP
0.4	36.9	50.0	21.1	50.1	51.1	28.8
0.8	40.5	53.6	35.8	52.3	53.3	28.8
1.2	40.4	63.1	85.4	62.5	58.8	32.2
1.6	100 (150 min)	63.1	100(150 min)	62.5	64.4	32.2
2.0	100 (120 min)	71.4	100 (120 min)	70.9	71.1	40.0

values also increased which might be attributed to the increase in number of surface active sites. The kinetic rate constant of dye solution was slightly lower than that in individual dye solution. The comparative rate constants for various dye degradation using bINP were more than that of cINP.

Online Co

The calculated DR % of RR238, RB235 and dye mix at different concentrations of bINP and cINP is given in Table 2. At 2.0 gl^{-1} concentration, INP catalyzed Fenton process resulted in the fastest degradation of RR238, RB235 and dye mix. The degradation efficiency of bINP (1.6 gl^{-1}) towards RR238 and RB235 was found to be 100% and that of cINP was found to be 70% and 71%, respectively. The removal of pure dye solutions appeared to be comparatively much better than that of mixture of dyes. Overall bINP appeared to be more effective than cINP as a Fenton like catalyst both in terms of extent and speed of dye removal.

Thus, *Syzygium cumini* leaf extract synthesized iron oxide nanoparticles were better catalysts than cINP for free radical production from H_2O_2. A possible reason is agglomeration of cINP during the synthesis and utilization process, whereas bINP were prevented from agglomerating by the effective capping activity of polyphenols present in *Syzygium cumini* leaf extract.

Fig. 8 shows the efficiency of INP catalyzed Fenton process to decolorize textile industry wastewater as determined from the periodic absorbance spectra collections (from 400-700 nm). bINP treated wastewater decolorized rapidly and the color completely disappeared at about 100 min, and cINP treated wastewater decolorized slowly, while the intensity of color showed no visible change after a contact time of 100 min. Similar trend was observed by Satapnajaru *et al*. (2011) in wastewater sample containing a variety of disperse, reactive azo dyes and other dyes treated by NZVI. Treatment of wastewater sample with bINP resulted in decolorization that was consistent with decolorization of azo dyes (Nam and Tratnyek, 2000).

bINP possess different morphology and structural characteristics than cINP. Results of dye decolorization studies revealed that bINP demonstrated faster kinetics and higher removal percentage of RR238, RB235, dye mix and wastewater from textile dyeing industry than cINP.

References

Arjunan, B. and M. Karuppan: A review on Fenton and improvements to the Fenton process for wastewater treatment. *J. Environ. Chem. Eng*., **2**, 557–572 (2014).

Bajpai, M., A. Pande, S.K. Tewari and D. Prakash: Phenolic contents and antioxidant activity of some food and medicinal plants. *Int. J. Food Sci. Nutr*., **56**, 287 (2005).

Bernal-Martinez, L.A., C. Barrera-Diaz, C. Solis-Morelos and N. Reyna: Synergy of electrochemical and ozonation processes in industrial wastewater treatment. *Chem. Eng. J*., **165**, 71–77 (2010).

Byung, H.M., B.P. Young and H.P. Kyung: Fenton oxidation of orange II by pre-reduction using nanoscale zero valent iron. *Desalination*, **268**, 249-252 (2011).

Carliell, C.M., S.J. Barclay, N. Naidoo, C.A. Buckley, D.A. Mulholland and E. Senior: Anaerobic decolorisation of reactive dyes in conventional sewage treatment process. *Water S.A*., **20**, 341-345 (1994).

Carliell, C.M., S.J. Barclay and C.A. Buckley: Treatment of exhausted reactive dye bath effluent using anaerobic digestion: laboratory and full scale trials. *Water S.A*., **22**, 225233 (1996).

Chang, M.C., H.Y. Shu, H.H. Yu and Y.C. Sung: Reductive decolourization and total organic carbon reduction of the diazo dye C.I. Acid Black 24 by zero-valent iron powder. *J.Chem. Technol. Biot*., **81**, 1259-1266 (2006).

Changha, Lee, Jee Yeon Kim, Won Il Lee, Kara, L. Nelson, Jeyong Yoon and David, L. Sedlak: Bactericidal Effect of Zero-Valent Iron Nanoparticles on *Escherichia coli*. *Environ. Sci. Technol*., **42(13)**, 4927–4933 (2008).

Eric, C.N., Hui Huang, Lisa Stafford, Homer Genuino, M.G. Hung, B.C. John, E.H. George and L.S. Steven: Biosynthesis of iron and silver nanoparticles at room temperature using aqueous Sorgham bran extracts. *Langmuir*, **27**, 64-271 (2011).

Frank, P. van der Zee and S. Villaverde: Combined anaerobic – aerobic treatment of azo dye-A short review of bioreactor studies. *Water Res*., **39**, 1425- 1440 (2005).

Garg, A., I.M. Mishra and S. Chand: Oxidative phenol degradation using non-noble metal based catalysts. *Clean*, **38**, 27–34 (2010).

Hung-Yee Shu, Ming-Chin Chang, Hsing-Hung Yu and Wang –Hung Chen: Reduction of an azo dye acid black 24 solution using synthesized nanoscale zerovalent iron particles. *J. Colloid Interf. Sci*., **314**, 89-97 (2007).

Krishnan, R. and G.B. Maru: Isolation and analyses of polymeric polyphenol fractions from black tea. *Food Chem.,* **94,** 331–340 (2006).

Máirtin, Ó., Astill, C. and S. Schumm: Potentiometric, FTIR and NMR studies of the complexation of metals with theaflavin. *Dalton T.,* **5**, 801–807 (2003).

Mukesh Chander, Dalijit Singh and Ramandeep Kaur: Biodecolorisation of reactive red an industrial dye by *Phlebia* spp. *J. Environ. Biol*., **35**, 1031-1036 (2014).

Nam, S. and P.G. Tratnyek: Reduction of azo dye with zero-valent iron. *Water Res*., **34**, 1837–184 5 (2000).

Nigam, P.: Textile effluent Decolorization and dye-adsorbed agricultural residue biodegradation. *Bioresource Technol*., **77**, 247-255 (2000).

Pinheiro, H.M., E. Touraud and O. Thomas: Aromatic amines from azo dye reduction: Status review with emphasis on direct UV spectrophotometric detection in textile industry wastewaters. *Dyes*, **61**, 121-139 (2004).

Rajkumar, S.A. and S. Nagan: Study on Tirupur CETPs discharge and their impact on Noyyal river and Orathupalayam dam, TamilNadu, India. *J. Environ. Res. Develop*. **5,** 558-565 (2011).

Sada Venkateswarlu, B. Natesh Kumar, C.H. Prasad, P. Venkateswarlu and N.V.V. Jyothi:Bio-inspired green synthesis of Fe_3O_4 spherical magnetic nanoparticles using Syzygium cumini seed extract. *Physica B*, **449**, 67-71 (2014).

Satapnajaru, T., C. Chompuchan, P. Suntornchaot and P. Pengthamkeerati: Enhancing decolrization of reactive black 5 and reactive red 198 during nano zerovalent iron treatment.

Online Copy

Desalination, **266**, 218-230 (2011).

Shahwan, T., S. Abu Sirriah, M. Nairata, E. Boyac, A.E. Eroglu, , T.B. Scott and K.R. Hallam: Green synthesis of iron nanoparticles and their application as a Fenton-like catalyst for the degradation of aqueous cationic and anionic dyes. *Chem. Eng. J*., **172**, 258– 266 (2011).

Siavash Iravani: Green synthesis of metal nanoparticles using plants. *Green Chem.*, **13,** 2638–2650 *(*2011).

Sun, Y.P., X.Q. Li, J. Cao, W.X. Zhang and H.P. Wang: Characterization of zero valent iron nanoparticles. *Adv. Colloid Interf. Sci*., **120**, 47-56 (2006).

Sun, Y.P., X.Q. Li, J. Cao, W.X. Zhang and H.P. Wang: A method for the preparation of stable dispersion of zero valent iron particles of decoloration of acid blue 113 azo dye solution. *J. Hazard. Mater*., **184**, 172-18 (2007).

Susanto, H., Y. Feng and M. Ulbricht: Fouling behavior of aqueous solutions of polyphenolic compounds during ultrafiltration. *J. Food Eng.,* **91,** 333–340 (2009).

Tang, W.Z. and R.Z. Chen: Decolorization kinetics and mechanisms of commercial dyes by H_2O_2/ iron powder system. *Chemosphere*, **32**, 947-958 (1996).

Venkatesh, S., A.R. Quaff and N.D. Pandey: Treatment and reuse of dye wastewater from the textile industry. A review of advanced treatment technologies. *Int. J. Adv. Res. Civil Struct. Environ. Infra. Eng. Develop.*, **4,** 1-9 (2011)**.**

Vineet Kumar, Subhash, C. Yadav and Sudesh Kumar Yadav: *Syzygium cumini* leaf and seed extract mediated biosynthesis of silver nanoparticles and their characterization. *J. Chem. Technol. Biotechnol.,* **85,** 1301–1309 **(**2010).

Willetts, J.R.M., N.J. Ashbolt, R.E. Moosbrugger and M.R. Aslam, : The use of a thermophilic anaerobic system for pretreatment of textile dye wastewater. *Water Sci. Technol*., **42,** 309–316 **(**2000**).**

Online Copy